ARMY RESEARCH LABORATORY

Visibility Factor and Polydispersity of the Light Scattering from Particles on Surfaces

Gorden Videen, J. L. de la Peña, J. M. Saiz, F. González, P. J. Valle, and F. Moreno

ARL-TR-2090   December 1999

20000118 161

Army Research Laboratory

Adelphi, MD 20783-1197

Visibility Factor and Polydispersity of the Light Scattering from Particles on Surfaces

Gorden Videen

Information Science and Technology Directorate, ARL

J. L. de la Peña, J. M. Saiz, F. González, P. J. Valle, and F. Moreno

Depto. Física Aplicada, Grupo de Optica, Universidad de Cantabria

Abstract

We have developed an experimental method based on the visibility factor of the light-scattering minima to obtain size-polydispersity information from contaminants on a flat substrate. We verify the method using double-interaction-model calculations and use this technique to experimentally examine the radial variation of a micrometer-sized fiber and the size polydispersity of spherical particles on a substrate.

Contents

Figures

1. Introduction

The detection and characterization of particles on flat surfaces has been a topic of increasing interest over the last several years because of its wide applicability in many fields of science and technology [1,2]. In general, particulate samples may contain contaminants of different size and shape. Here, we use the far-field light scattered from contaminated substrates to characterize the size polydispersity of the contaminants. From visibility measurements of the minima of the S-polarized scattered light, we can obtain an estimate of the upper limit of the size polydispersity. To our knowledge this is the first time that polydispersity has been measured by this means. We verify the method experimentally using two fundamentally different samples: a substrate contaminated by a polydispersion of spheres and a cylinder lying on a substrate.

2. Solution and Results

We consider spherical or cylindrical contaminants having small size poly-dispersity in radius R. This kind of sample can be characterized by a probability density function (PDF) $p(R)$ with mean value R_o and degree of size polydispersity r defined as the ratio between the square root of the variance σ and R_o. We assume a low density of contaminants and little or no aggregation, such that the interaction between individual contaminants is negligible. The total scattered intensity received at scattering angle θ_s is obtained by

$$\langle I(R, \theta_s) \rangle = \int_0^\infty I(R, \theta_s) p(R, R_o, r) \ dR \ , \tag{1}$$

where $I(R, \theta_s)$ is the scattered intensity at angle θ_s by a contaminant of radius R illuminated at normal incidence. The scattering angle θ_s is measured from the normal to the substrate.

Analysis of equation (1) requires information about the scattering intensities $I(R, \theta_s)$. For normal-incidence illumination, we empirically find that the scattered intensities can be approximated by

$$I(R, \theta_s) = A \left\{ 1 - \cos \left[k\gamma R \left(\theta_s - \frac{\pi}{2} \right) \right] \right\} \ , \tag{2}$$

where A is a normalization factor, $k = 2\pi/\lambda$, and γ is a fitting parameter. For the samples we analyzed (gold-coated spheres and cylinders on gold substrates), $\gamma = 3.3$ produces adequate results. Figure 1 shows how this expression reproduces the main characteristics (lobed structure and angular positions of minima) of the S-polarized far-field scattering pattern from a cylinder on a plane substrate. We obtain experimental results using the technique described by González et al [3]. Theoretical results are calculated with a modified version [4–6] of the Nahm-Wolfe double interaction model [7], which displays the same general features obtained by other more accurate techniques [8–10].

It is highly desirable to choose a PDF that is both analytical and realistic. The gamma function is considered valid for both high- and low-polydispersity regimes [11]:

$$p(R)dR = \frac{a^m R^{m-1} \exp(-aR)}{\Gamma(m)} dR \ , \tag{3}$$

Figure 1. Experimental (circles), double-interaction model [5] (line), and empirical approximation (dashed) S-polarized light-scattering intensity from a cylinder ($R/\lambda = 0.87$) on a substrate (both gold coated: $\hat{\epsilon} = -11 + 1.5i$) illuminated at normal incidence.
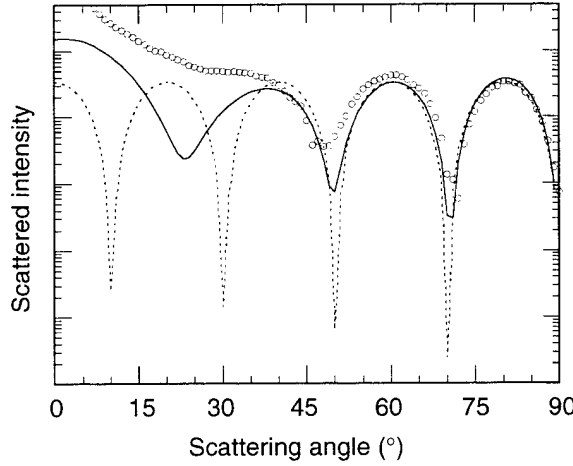
where the parameters a and m are defined as $a = R_o \sigma^{-2}$ and $m = r^{-2}$. Substituting the expressions of equations (2) and (3) allows equation (1) to be integrated, providing an analytical approximation for $\langle I\,(R, \theta_s) \rangle$:

$$\langle I\,(R, \theta_s) \rangle \approx A - \frac{A \cos\left\{ \frac{1}{r^2} \arctan\left[r^2 k \gamma R_o \left(\theta_s - \frac{\pi}{2} \right) \right] \right\}}{\left\{ 1 + \left[k \gamma R_o r^2 \left(\theta_s - \frac{\pi}{2} \right) \right]^2 \right\}^{1/2r^2}}. \tag{4}$$

The above expression approximates the scattered intensities from substrates contaminated by polydispersities of spheres or cylinders. This study focuses on samples having small size polydispersities, i.e., r is smaller than approximately 0.1 (10 percent). For contaminant sizes on the order of the wavelength, the cosine argument may be approximated by $k\gamma R_o(\theta_s - \frac{\pi}{2})$, and the angular frequency of the scattered intensity is now approximately proportional to the mean value R_o:

$$\langle I\,(\theta_s) \rangle \approx A - \frac{A \cos\left[k \gamma R_o \left(\theta_s - \frac{\pi}{2} \right) \right]}{\left\{ 1 + \left[k \gamma R_o r^2 \left(\theta_s - \frac{\pi}{2} \right) \right]^2 \right\}^{1/2r^2}}. \tag{5}$$

The denominator in equation (5) is slowly varying, so the angular positions of the minima and maxima are nearly independent of the degree of polydispersity r. Figure 2 (a) shows the scattered intensities predicted by equation (5), and figure 2 (b) shows those predicted by the use of a modified version of the double-interaction model [5,6] for a polydisperse sample of mean relative value $R_o/\lambda = 2.53$ ($R_o = 1.6\ \mu$m; $\lambda = 0.6328\ \mu$m); $r = 3$, 6, and 9 percent. Parameter A is chosen as unity. The order m of the lobes is numbered from $m = 0$, corresponding to the maximum/minimum observed nearest the grazing angles. Higher values of m correspond to the successive lobes observed at scattering angles toward the specular direction.

3

Figure 2. (a) Empirical and (b) double-interaction model predictions of a light-scattering intensities from low size polydisperse spherical particles on a substrate illuminated at normal incidence. The mean relative value is $R_o/\lambda = 2.53$ and the angular resolution is $1°$. Mean relative value is $R_o/\lambda = 2.53$ and angular resolution is $1°$. Dots line: monodisperse sample; continuous line: $r = 3$ percent; dashed line: $r = 6$ percent.
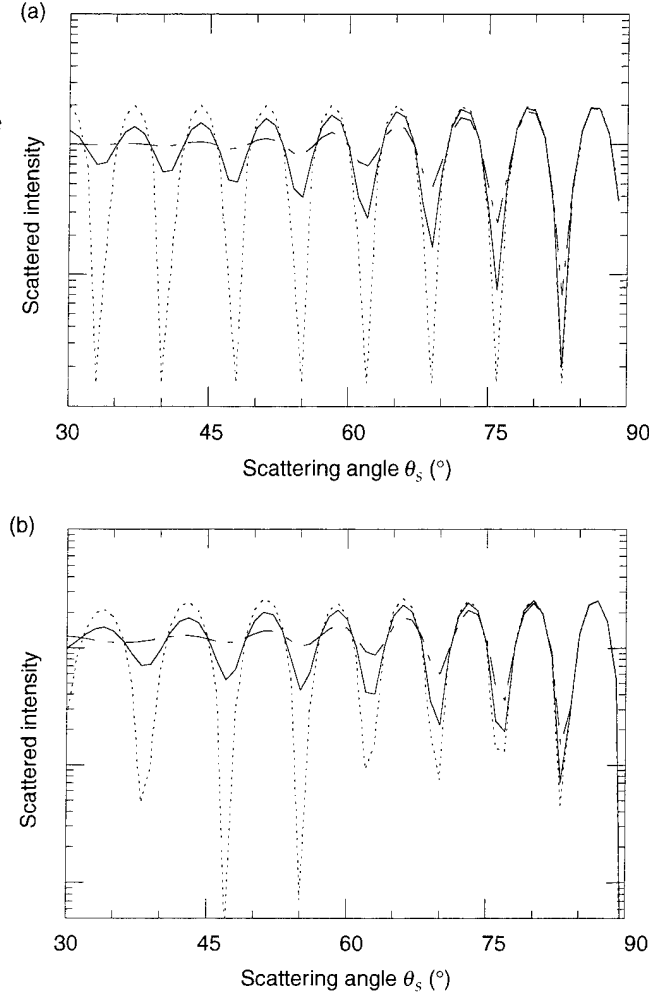
Samples with different degrees of polydispersity have been analyzed theoretically and similar behavior has been found in all cases. As the sample becomes more polydisperse, a smoothing of the lobed structure occurs (fig. 2), i.e., the minima become more shallow. The difference between the maximum and minimum intensities is very sensitive to changes in the degree of polydispersity r. The amount of smoothing also depends on the angular positions of the minima. Those minima of highest order, closest to specular, disappear most rapidly. We can quantify this connection between a feature in the light-scattering pattern and a characteristic parameter of the polydispersity using the visibility factor $V(m)$, defined for each lobe of order m as

$$V(m) = \frac{\langle I\left(\theta_s^{\max}, R_o, r\right)\rangle - \langle I(\theta_s^{\min}, R_o, r)\rangle}{\langle I\left(\theta_s^{\max}, R_o, r\right)\rangle + \langle I(\theta_s^{\min}, R_o, r)\rangle} \;, \tag{6}$$

4

where θ_s^{max} and θ_s^{min} are the angular positions corresponding to the maximum and the minimum intensities of the lobe of order m. If a parameter β_s is defined as

$$\beta_s = \left\{ 1 + \left[k\gamma R_o \left(\theta_s - \frac{\pi}{2} \right) r^2 \right]^2 \right\}^{-1/2r^2} , \qquad (7)$$

then from equation (6) we obtain

$$V(m) \approx \frac{\beta_s^{\mathrm{max}} + \beta_s^{\mathrm{min}}}{2 + \beta_s^{\mathrm{max}} - \beta_s^{\mathrm{min}}} , \qquad (8)$$

where the superscripts refer to a minimum or maximum. Note that for particles with relative size well above the wavelength, the angular positions of a minimum approach that of their corresponding maximum ($\beta_s^{\mathrm{max}} \approx \beta_s^{\mathrm{min}}$), resulting in the simple expression $V(m) \approx \beta_s^{\mathrm{min}}$. This equation also holds quite well for smaller size particles, i.e., particles whose sizes are on the order of the wavelength. In a previous work [4–6], an expression was developed relating the particle size to the angular positions of the mth minima:

$$\left(\theta_s^{\mathrm{min}} - \frac{\pi}{2} \right) \approx -\frac{\alpha(m)}{2R_o} \text{ with } \alpha(m) \approx 0.292 + 0.316m. \qquad (9)$$

We can now approximate the visibility factor by

$$V(m) \approx \beta_s^{\mathrm{min}} \approx \left\{ 1 + \left[2\pi\gamma\alpha(m) r^2 \right]^2 \right\}^{-1/2r^2} . \qquad (10)$$

For each r, the visibility decreases as the order increases, independent of R_o. This means that, although different samples with the same polydispersity r produce quite different light-scattering patterns, minima of the same order m have the same visibility.

We now compare the predictions of $V(m)$ and experimental data obtained from two fundamentally different samples. The first sample consists of a dilute set of spherical latex particles seeded on a flat substrate and metalized by means of a gold-sputtering process [3]. The nominal radius of the spheres before coating is $R = 1.594 \pm 0.027$ μm ($r = 1.7$ percent). The second sample consists of a single fiber of nominal radius $R \approx 0.55$ μm, placed on a substrate and metalized in the same way. The fiber is not uniform, but has a secondary ripple that is approximately sinusoidal and causes the radius to vary by a few percent over millimeter-size length scales. We measured the S-polarized scattering intensities using the apparatus and technique described by González et al [3]. From these intensities, we can determine the visibility of the minima. The illumination area on the sample

containing the cylinder is larger than the length scale of the ripple structure on the sample.

Figure 3 shows the evolution of the visibility factor $V(m)$ predicted by equation (10). Superimposed on this plot are measured visibilities for the sample of spheres on a substrate and for the fiber on a substrate. Depending on the mean size of the contaminants, the number of minima change and only that number of points are available for comparison with theory. We expect the experimentally measured visibilities to follow one of the trajectories, and this occurs for the substrate containing the cylinder. The trajectory, followed by the points for the cylinder, corresponds to a size polydispersity of approximately $r = 4$ percent, which is in agreement with estimates made by the manufacturers.

For the polydispersion of spheres on the substrate, the experimentally measured visibilities do not follow any of the trajectories. The reason for this is that size polydispersity is not the only cause for the loss of visibility. Shape polydispersity, microirregularities on the substrate, high surface densities, and the presence of particle clusters all contribute to a loss of visibility. The existence of some of these effects in the sample can significantly alter the visibility of some minima, even the angular minima positions themselves [13–15]. Photomicrographs of similar samples [3,12] show such clustering and other microcontaminants that can cause a loss of visibility. Because the sample containing the fiber consists of only one primary scattering particle, some of the effects we mentioned above are not present, and the experimental evolution of $V(m)$ displays better agreement with the analytical predictions for the existing orders ($m = 0,1$).

Figure 3. Evolution of $V(m)$ for some values of r (expressed as percentage) by means of equation (10). Circles correspond to measurable points. Experimental visibilities for a substrate with spherical particles (triangles) and a substrate with a fiber (squares) are shown. Arrows show minimum value of r by any order for a given sample (see text).
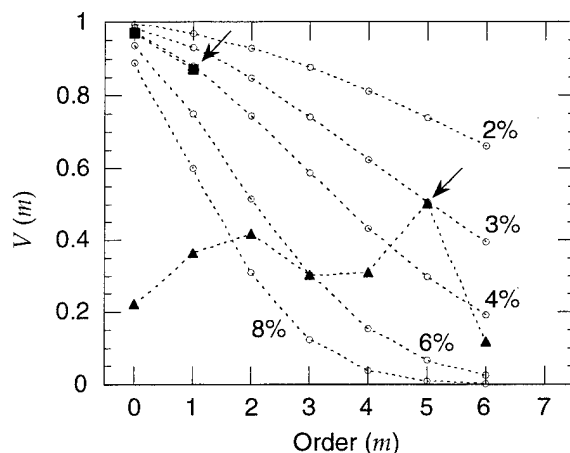
3. Conclusion

More analysis is necessary for the sample of spheres on a substrate. It is known that high-visibility minima are more sensitive than low-visibility minima. The experimental points on the $V(r)$ curves corresponding to the lowest values of r (those farthest to the right on the graph) are the minima whose visibility is least affected by these other factors. Therefore, the polydispersity corresponding to these minima more closely agrees with the actual polydispersity. The polydispersity constitutes an upper-limit estimate of the maximum size polydispersity of the sample. For the spheres, the lobe of order $m = 5$ has a visibility of $V(r) = 0.50$, corresponding to a size polydispersity of about $r = 3$ percent. This estimate agrees, as an upper limit, with the initial value of the nominal radius of the sample ($r \approx 1.7$ percent). Four different spots in the sample have been measured, yielding similar results.

References

1. P. Lilienfeld, *Aerosol Sci. Technol.* **5**, 145 (1986).

2. M. L. Liswith, E. J. Bawolek, and E. D. Hirleman, *Opt. Eng.* **35**, 858 (1996).

3. F. González, J. M. Saiz, P. J. Valle, and F. Moreno, *Opt. Commun.* **137**, 359 (1997).

4. F. Moreno, J. M. Saiz, P. J. Valle, and F. González, *Appl. Phys. Lett.* **68**, 3087 (1996).

5. J. L. de la Peña, F. González, J. M. Saiz, F. Moreno, and P. J. Valle, *J. Appl. Phys.* **85**, 432 (1999).

6. J. L. de la Peña, J. M. Saiz, P. J. Valle, F. González, and F. Moreno, *Part. Syst. Charact.* **16**, 1 (1999).

7. K. B. Nahm and W. L. Wolfe, *Appl. Opt.* **26**, 2995 (1987).

8. B. R. Johnson, *J. Opt. Soc. Am. A*, **9**, 1341 (1992); errata, *J. Opt. Soc. Am. A* **10**, 766 (1993).

9. G. Videen, *J. Opt. Soc. Am. A* **8**, 483 (1991); errata, *J. Opt. Soc. Am. A* **9**, 844 (1992).

10. G. Videen, *Opt. Commun.* **115**, 1 (1995).

11. T. Allen, *Particle Size Measurements, Volume 1*, 5th ed., Chapman & Hall (1997).

12. J. M. Saiz, P. J. Valle, F. González, and F. Moreno, *Opt. Eng.* **33**, 1261 (1994).

13. F. González, J. M. Saiz, P. J. Valle, and F. Moreno, *Opt. Eng.* **34**, 1200 (1995).

14. P. J. Valle, F. Moreno, J. M. Saiz, and F. González, *IEEE Trans. Antennas Propag.* **44**, 321 (1996).

15. Yu-lin Xu, *Appl. Opt.* **36**, 9496 (1997).

Distribution

Admnstr
Defns Techl Info Ctr
Attn DTIC-OCP
8725 John J Kingman Rd Ste 0944
FT Belvoir VA 22060-6218

Central Intllgnc Agency Dir DB Standard
Attn OSS/KPG/DHRT
1E61 OHB
Washington DC 20505

Dir of Defns Rsrch & Engrg
Attn DD TWP
Attn Engrg
Washington DC 20301

Ofc of the Secy of Defns
Attn ODDRE (R&AT)
The Pentagon
Washington DC 20301-3080

OSD
Attn OUSD(A&T)/ODDR&E(R) R J Trew
Washington DC 20301-7100

Commanding Officer
Attn NMCB23
6205 Stuart Rd Ste 101
FT Belvoir VA 22060-5275

AMCOM MRDEC
Attn AMSMI-RD W C McCorkle
Redstone Arsenal AL 35898-5240

CECOM
Attn PM GPS COL S Young
FT Monmouth NJ 07703

Dir for MANPRINT
  Ofc of the Deputy Chief of Staff for Prsnnl
Attn J Hiller
The Pentagon Rm 2C733
Washington DC 20301-0300

Dir of Chem & Nuc Ops DA DCSOPS
Attn Techl Lib
Washington DC 20301

TECOM
Attn AMSTE-CL
Aberdeen Proving Ground MD 21005-5057

US Army Armament Rsrch Dev & Engrg Ctr
Attn AMSTA-AR-TD M Fisette
Bldg 1
Picatinny Arsenal NJ 07806-5000

US Army Edgewood RDEC
Attn SCBRD-TD G Resnick
Aberdeen Proving Ground MD 21010-5423

US Army Engrg Div
Attn HNDED FD
PO Box 1500
Huntsville AL 35807

US Army Info Sys Engrg Cmnd
Attn ASQB-OTD F Jenia
FT Huachuca AZ 85613-5300

US Army Natick RDEC Acting Techl Dir
Attn SSCNC-T P Brandler
Natick MA 01760-5002

US Army NGIC
Attn Rsrch & Data Branch
220 7th Stret NE
Charlottesville VA 22901-5396

US Army Nuc & Cheml Agency
7150 Heller Loop Ste 101
Springfield VA 22150-3198

US Army Simulation, Train, & Instrmntn
  Cmnd
Attn J Stahl
12350 Research Parkway
Orlando FL 32826-3726

US Army Strtgc Defns Cmnd
Attn CSSD H MPL Techl Lib
PO Box 1500
Huntsville AL 35807

Distribution (cont'd)

US Army Tank-Automtv Cmnd Rsrch, Dev,
  & Engrg Ctr
Attn AMSTA-TA J Chapin
Warren MI 48397-5000

US Army Train & Doctrine Cmnd Battle Lab
  Integration & Techl Dirctrt
Attn ATCD-B J A Klevecz
FT Monroe VA 23651-5850

US Military Academy
Mathematical Sci Ctr of Excellence
Attn MDN-A LTC M D Phillips
Dept of Mathematical Sci Thayer Hall
West Point NY 10996-1786

Dept of the Navy Chief of Nav OPS
Attn OP 03EG
Washington DC 20350

Nav Surface Warfare Ctr A
Attn Code B07 J Pennella
17320 Dahlgren Rd Bldg 1470 Rm 1101
Dahlgren VA 22448-5100

DARPA
Attn S Welby
Attn Techl Lib
3701 N Fairfax Dr
Arlington VA 22203-1714

US Dept of Energy
Attn KK 22 K Sisson
Attn Techl Lib
Washington DC 20585

Hicks & Associates Inc
Attn G Singley III
1710 Goodrich Dr Ste 1300
McLean VA 22102

Director
US Army Rsrch Ofc
4300 S Miami Blvd
Research Triangle Park NC 27709

Army Rsrch Ofc
Attn AMSRL-RO-EN Bach
PO Box 12211
Research Triangle Park NC 27709

US Army Rsrch Lab
Attn AMSRL-CI-AS Mail & Records Mgmt
Attn AMSRL-CI-AT Techl Pub (3 copies)
Attn AMSRL-CI-LL Techl Lib (3 copies)
Attn AMSRL-DD J Rocchio
Attn AMSRL-IS-EE G Videen (3 copies)
2800 Powder Mill Rd
Adelphi MD 20783-1197

REPORT DOCUMENTATION PAGE

Public reporting burden for this collection of information is estimated to average 1 hour per response, including the time for reviewing instructions, searching existing data sources, gathering and maintaining the data needed, and completing and reviewing the collection of information. Send comments regarding this burden estimate or any other aspect of this collection of information, including suggestions for reducing this burden, to Washington Headquarters Services, Directorate for Information Operations and Reports, 1215 Jefferson Davis Highway, Suite 1204, Arlington, VA 22202-4302, and to the Office of Management and Budget, Paperwork Reduction Project (0704-0188), Washington, DC 20503.

1. AGENCY USE ONLY *(Leave blank)*	2. REPORT DATE December 1999	3. REPORT TYPE AND DATES COVERED Final, January to February 1999

4. TITLE AND SUBTITLE Visibility Factor and Polydispersity of the Light Scattering from Particles on Surfaces

5. FUNDING NUMBERS

DA PR: B53A

PE: 61102A

6. AUTHOR(S) Gorden Videen (ARL), J. L. de la Peña, J. M. Saiz, F. González, P. J. Valle, and F. Moreno (Depto. Física Aplicada, Grupo de Optica, Universidad de Cantabria)

7. PERFORMING ORGANIZATION NAME(S) AND ADDRESS(ES)
U.S. Army Research Laboratory
Attn: AMSRL-IS-EM   email: gvideen@arl.mil
2800 Powder Mill Road
Adelphi, MD 20783-1197

8. PERFORMING ORGANIZATION REPORT NUMBER
ARL-TR-2090

9. SPONSORING/MONITORING AGENCY NAME(S) AND ADDRESS(ES)
U.S. Army Research Laboratory
2800 Powder Mill Road
Adelphi, MD 20783-1197

10. SPONSORING/MONITORING AGENCY REPORT NUMBER

11. SUPPLEMENTARY NOTES
ARL PR: 7FEJ70
AMS code: 61110253A11

12a. DISTRIBUTION/AVAILABILITY STATEMENT Approved for public release; distribution unlimited.

12b. DISTRIBUTION CODE

13. ABSTRACT *(Maximum 200 words)*

We have developed an experimental method, based on the visibility factor of the light-scattering minima, to obtain size-polydispersity information from contaminants on a flat substrate. We verify this method using double-interaction-model calculations and use this technique to experimentally examine the radial variation of a micrometer-sized fiber and the size polydispersity of spherical particles on a substrate.

14. SUBJECT TERMS
Scattering, visibility

15. NUMBER OF PAGES
18

16. PRICE CODE

17. SECURITY CLASSIFICATION OF REPORT Unclassified	18. SECURITY CLASSIFICATION OF THIS PAGE Unclassified	19. SECURITY CLASSIFICATION OF ABSTRACT Unclassified	20. LIMITATION OF ABSTRACT SAR

NSN 7540-01-280-5500